# Determining Sources of Dissolved Organic Carbon and Disinfection Byproduct Precursors to the McKenzie River, Oregon

**Tamara E. C. Kraus* and Chauncey A. Anderson** USGS
**Karl Morgenstern** Eugene Water and Electric Board
**Bryan D. Downing, Brian A. Pellerin, and Brian A. Bergamaschi** USGS

This study was conducted to determine the main sources of dissolved organic carbon (DOC) and disinfection byproduct (DBP) precursors to the McKenzie River, Oregon (USA). Water samples collected from the mainstem, tributaries, and reservoir outflows were analyzed for DOC concentration and DBP formation potentials (trihalomethanes [THMFPs] and haloacetic acids [HAAFPs]). In addition, optical properties (absorbance and fluorescence) of dissolved organic matter (DOM) were measured to provide insight into DOM composition and assess whether optical properties are useful proxies for DOC and DBP precursor concentrations. Optical properties indicative of composition suggest that DOM in the McKenzie River mainstem was primarily allochthonous—derived from soils and plant material in the upstream watershed. Downstream tributaries had higher DOC concentrations than mainstem sites (1.6 ± 0.4 vs. 0.7 ± 0.3 mg $L^{-1}$) but comprised <5% of mainstem flows and had minimal effect on overall DBP precursor loads. Water exiting two large upstream reservoirs also had higher DOC concentrations than the mainstem site upstream of the reservoirs, but optical data did not support in situ algal production as a source of the added DOC during the study. Results suggest that the first major rain event in the fall contributes DOM with high DBP precursor content. Although there was interference in the absorbance spectra in downstream tributary samples, fluorescence data were strongly correlated to DOC concentration ($R^2$ = 0.98), THMFP ($R^2$ = 0.98), and HAAFP ($R^2$ = 0.96). These results highlight the value of using optical measurements for identifying the concentration and sources of DBP precursors in watersheds, which will help drinking water utilities improve source water monitoring and management programs.

The implementation of stricter regulations for disinfection byproducts (DBPs) has highlighted the need to understand the sources of DBP precursors to drinking water intakes. DBPs are generated during drinking water treatment (e.g., chlorination and ozonation) when components of the organic matter pool, both dissolved and particulate, react to form halogenated compounds. Several DBPs, including trihalomethanes (THMs) and haloacetic acids (HAAs), have been shown to be carcinogenic and mutagenic (Leenheer and Croué, 2003). Concentrations of DBPs in distribution systems are reflective of both source water quality and treatment plant operations. Identifying sources of DBP precursors will enable utilities to implement effective, targeted watershed management strategies to reduce DBPs in their distribution system. For example, understanding DBP sources allows for planning of treatment options in relation to seasonal trends, as well as long-term changes in land use and climate. For many utilities, source water protection programs that lower the amount of DBP precursors entering water treatment plants may be more feasible and cost effective than implementing additional water treatment technologies (Aiken and Cotsaris, 1995; Stepczuck et al., 1998, Reckhow et al., 2004).

The DBP precursor pool is a subset of the bulk organic matter (OM) pool. Watershed sources of OM include decomposing OM leaching out of soils by both surface and groundwater flow; leaching of fresh and senescing plant material; algal production within the water column; and anthropogenic sources such as domestic sewage. The amount and reactivity of OM that arrives at a drinking water intake is a function of the amount and composition of OM entering the water throughout the watershed, as well as environmental processes (e.g., biodegradation, photodegradation, and sorption)

Copyright © 2010 by the American Society of Agronomy, Crop Science Society of America, and Soil Science Society of America. All rights reserved. No part of this periodical may be reproduced or transmitted in any form or by any means, electronic or mechanical, including photocopying, recording, or any information storage and retrieval system, without permission in writing from the publisher.

J. Environ. Qual. 39:2100–2112 (2010)
doi:10.2134/jeq2010.0030
Published online 25 Aug. 2010.
Supplemental data file available online for this article.
Received 22 Jan. 2010.
*Corresponding author (tkraus@usgs.gov).
© ASA, CSSA, SSSA
5585 Guilford Rd., Madison, WI 53711 USA

T.E.C. Kraus, B.D. Downing, B.A. Pellerin, and B.A. Bergamaschi, USGS–California Water Science Center, Sacramento, CA 95819; C.A. Anderson, USGS–Oregon Water Science Center, Portland, OR 97201; K. Morgenstern, Eugene Water and Electric Board, Eugene, OR 97440. Assigned to Associate Editor Robert Cook.

**Abbreviations**: $A_{254}$, ultraviolet absorbance at 254 nm; DBP, disinfection byproduct; DBPFP, disinfection byproduct formation potential; DOC, dissolved organic carbon; DOM, dissolved organic matter; EEM, excitation-emission matrix; EWEB, Eugene Water and Electric Board; FDOM, fluorescent dissolved organic matter; FI, fluorescence index; HAA, haloacetic acid; HAAFP, haloacetic acid formation potential; MRBO, McKenzie River above the South Fork; OM, organic matter; PARAFAC, parallel factor analysis; PC, principle component; PCA, principle component analysis; POC, particulate organic carbon; RM, river mile; $S_{275-295}$, spectral slope; SHAAFP, specific haloacetic acid formation potential; STHMFP, specific trihalomethane formation potential; SUVA, specific ultraviolet absorption; THM, trihalomethane; THMFP, trihalomethane formation potential; TOC, total organic carbon; VIDA, mainstem site located downstream of the two reservoir inflows.

that occur during transport. The transport and processing of this material is a function of land use, climate, hydrology, and management (Reckhow et al., 2004; Kraus et al., 2008; Engelage et al., 2009). For example, storm events can mobilize OM from decomposing litter and surface soils; agricultural practices can affect nutrient loads; and reservoir management can impact downstream OM concentration and composition. Thus, these processes influence drinking water quality.

Drinking water providers routinely measure total organic carbon (TOC) concentrations in raw and finished water to assess the effectiveness of the coagulation and filtration processes. To meet USEPA regulations, providers also measure distribution system DBP concentrations at least quarterly. However, because samples are not explicitly collected to monitor changes in source water quality, and because modifications to treatment plant operations affect the concentrations of TOC and DBPs in finished water, these data are usually insufficient to pick up event-based, seasonal, or long-term changes in water quality that can be linked to watershed processes. On the McKenzie River in Oregon, the Eugene Water and Electric Board (EWEB) provides drinking water to approximately 200,000 people. Although EWEB's raw water TOC levels and distribution system THM and HAA concentrations are significantly less than USEPA limits, elevated DBP concentrations occurred in EWEB's distribution system between 2005 and 2007, relative to earlier periods. It was unclear whether DBP levels would continue to rise. These observed increases coincided with the refilling of a large upstream reservoir that was previously drained to modify the withdrawal structures, as well as several changes in treatment plant operations (Anderson, 2007; HDR Engineering, 2007). The current study was undertaken as a proactive approach to source water protection in the watershed.

For many years, the drinking water industry has recognized the application of absorbance measured at 254 nm ($A_{254}$) as a proxy for dissolved organic carbon (DOC) concentration (Henderson et al., 2009). However, recent studies have also highlighted the use of dissolved organic matter (DOM) fluorescence measurements as a relatively rapid, less expensive, and potentially more accurate alternative to predict the concentration of DOC and DBP precursors (e.g., Coble, 2007; Hua et al., 2007; Hudson et al., 2007; Henderson et al., 2009). While absorbance spectroscopy measures the quantity of light absorbed by a water sample, fluorescence spectroscopy measures longer wavelength light that is emitted following absorption (Stedmon et al., 2003). The three-dimensional, excitation–emission matrices (EEMs) obtained from fluorescence spectroscopy also provide greater information about the chemical components of a given sample and qualitative information about the DOM pool (Coble, 2007; Hudson et al., 2007; Stedmon and Bro, 2008). Differences in the chemical makeup of the DOM pool can then be linked to changes in DOM reactivity, as well as being used to infer DOM source (e.g., McKnight et al., 2001; Stedmon et al., 2003; Spencer et al., 2007a,b; Jaffe et al., 2008).

This study, conducted by USGS in collaboration with EWEB, was initiated (i) to investigate watershed sources of DOC and DBP precursors to the McKenzie River, and (ii) to determine the usefulness of using optical measurements as proxies for DOC and DBP precursor concentrations. We also investigated the potential role of reservoirs for generating DOC and DBP precursor materials. Samples from mainstem sites of the McKenzie River, reservoir outflows, and tributary inputs were collected between August 2007 and March 2008, and analyzed for DOC and particulate organic carbon (POC) concentrations, absorbance, and fluorescence, as well as THM and HAA formation potentials (THMFP and HAAFP, respectively). These findings will help drinking water utilities improve source water monitoring and management programs in large watersheds.

## Materials and Methods

### Site Description

The Eugene Water and Electric Board supplies drinking water to approximately 200,000 people in Eugene, OR (USA). The sole source of this water is the McKenzie River, a 138-km-long tributary of the Willamette River (Supplemental Fig. S1). The McKenzie River drains a watershed of approximately 3460 $km^2$, with forested lands comprising the large majority of the watershed area—predominantly in the upper reaches and upland areas. Several small communities and agricultural land (primarily orchards, nurseries, row crops, and pastureland) are located in alluvial areas near the valley floor along several reaches. The adjacent cities of Springfield and Eugene, OR (combined population is approximately 340,000), are located near the mouth. The Eugene Water and Electric Board's drinking water intake is located at river mile (RM) 11, within the Springfield city limits.

The hydrology of the McKenzie River is dominated by discharge from the High Cascades geologic province in the upper reaches of the watershed. An important feature is the large, headwater springs that provide high, steady flows throughout the year (Sherrod and Smith, 2000, Tague and Grant, 2004). The Western Cascades geologic province, which comprises the middle and lower elevations, is heavily forested with streamflows that are determined more by rainfall runoff than snowmelt or groundwater. Following rainfall patterns, highest discharges occur in the winter with low flows in the dry summer and fall.

Two flood control reservoirs operated by the Army Corps of Engineers, Cougar and Blue River, are located in the Western Cascades on the South Fork McKenzie and Blue River, respectively. Cougar Reservoir has a storage capacity of $2.7 \times 10^8$ $m^3$ and catchment area of 509 $km^2$; and Blue River Reservoir has a storage capacity of $1.1 \times 10^8$ $m^3$ and catchment area of 227 $km^2$ (Johnson et al., 1995). The Cougar Reservoir was drained from 2002 to 2004 to modify the withdrawal structure to allow multilevel withdrawals for enhanced control of temperatures in the released water. During the drawdown period, vegetation grew on the exposed bed material and was subsequently inundated when the reservoir was refilled (Anderson, 2007). The primary inflow to Cougar Reservoir is the South Fork McKenzie River, which heads toward the High Cascades and includes at least one major spring source (Jefferson, 2006). Inflows to the Blue River Reservoir come entirely from Western Cascades streams. Aside from the upper McKenzie River springs, withdrawals from these two reservoirs are the largest source of water to the McKenzie River during low flows in summer and fall. Outflows from the Cougar Reservoir contribute about 10 to 35% of mainstem flows, whereas the Blue River Reservoir contributes about 5 to 20%. Because residence times in the reservoirs can be several months in the summer, DOM in water exiting these impound-

ments represents a mixture of material that has entered the reservoir over time as well as any in-reservoir processing (i.e., additions, losses, transformations).

Downstream from the South Fork McKenzie and Blue River, the hydrology and landscape become increasingly engineered. Two major diversions put up to 70 $m^3 s^{-1}$ or about 60% of summer flows into large canals for hydroelectric power production in Leaburg (RM 34.2) and Walterville (RM 24). In-stream discharges remaining in the McKenzie River are reduced to 30 $m^3 s^{-1}$ to comply with minimum flow requirements, until the return flows from the Walterville Canal enter the river at RM 17. Additional inflows in the reaches between the Walterville Canal and EWEB's intake include relatively small tributaries with runoff from agricultural and urban areas. Despite the influence of reservoirs, consumptive withdrawals, multiple smaller tributaries, and urban runoff, water in the McKenzie River at EWEB's intake generally has exceptional quality due to dilution effects from the strong influence of the headwater springs in the basin's upper reaches.

## Water Quality Sampling and Analyses

To assess the amount and character of DOM entering the McKenzie River, samples were collected from four sites along the mainstem of the river including water entering the EWEB drinking water treatment plant (intake), from the two tributaries representing reservoir inflows, and from three tributaries located between the reservoirs and intake (Table 1, Supplemental Fig. S1). Samples were collected over a 1- to 2-d period following a synoptic sampling approach. Samples were collected from five sites in August 2007 and all nine sites in September 2007, November 2007, and March 2008. Also, one water sample was collected from the intake in January 2008.

**Table 1. Descriptions of sampling locations.†**

| Site abbreviation (classification) | Site description | Water Source/Land Use | River mile (RM) | Flow range ($m^3 s^{-1}$)‡ | Latitude and longitude |
|---|---|---|---|---|---|
| MRBO (mainstem) | McKenzie River above the South Fork | Primarily groundwater entering via springs in the High Cascades. National forest managed by USFS, some commercial forestry, recreation, roads, and a few small communities. | 57.4 | 28–280 | Lat 44° 09′59″, Long 122° 15′19 ″ Lat 44° 09′59″, Long 122° 15′19″ |
| CGRO (reservoir inflow) | South Fork of the McKenzie below Cougar Reservoir | Primarily groundwater entering via springs in the High Cascades. Predominantly alpine and national forestland mixed with some commercial forestland. | 55.0 | 8–85 | Lat 44° 08′10″, Long 122° 14′50″ |
| BLUE (reservoir inflow) | Tributary site below Blue River Reservoir | Predominantly small streams originating in the Western Cascades. Land use same as CGRO; site is located downstream from the small community of Blue River. | 52.3 | 1.5–85 | Lat 44° 09′45″, Long 122° 19′55″ |
| VIDA (mainstem) | Mainstem site located downstream of the two reservoir inflows | Represents the summed inflows from MRBO, CGRO, and BLUE, in addition to inflows from Quartz Creek, a small Western Cascades tributary. Increased commercial forestland and several small communities. | 43.1 | 55–340 | Lat 44° 07′30″, Long 122° 28′10″ |
| HOLDEN (H) (mainstem) | Mainstem site at Holden Bridge, between the Leaburg and Walterville canals | Represents the entire mainstem flow between the locations of return flow from the Leaburg Canal and the diversion for the Walterville Canal. Increased development on river; two fish hatcheries, commercial forestland, and filbert orchards. | 27.2 | 28–395 | Lat 44° 5′23 ″, Long 122° 42′56″ |
| HENDRICKS (H) (mainstem) | Mainstem site below the Walterville Canal | Dewatered portion of the river as a result of the Walterville Canal diversion. Increased agriculture along valley floor (pasture, row crops, filberts, grass seed, etc.). | 20.1 | 55–395 | Lat 44° 03′21 ″, Long 122° 49′46″ |
| CAMP (tributary inflow) | Camp Creek tributary entering the mainstem in the lower valley floor | Extensive commercial forestry in the upper elevations and moderate agricultural and rural residential lands in the lower elevations; experiencing increasing development in the lower part of the basin. | 17.0 | 0.3–8.5 | Lat 44° 04′14 ″, Long 122° 53′05″ |
| CEDAR (tributary inflow) | Cedar Creek tributary entering the mainstem in the lower valley floor | Drains primarily urban residential lands, with forested headwaters; also receives storm drain contributions. | 14.1 | 0.03–7 | Lat 44° 03′34 ″, Long 122° 55′07″ |
| KEIZER (tributary inflow) | Urban runoff slough | Primarily receives its water from the mainstem of the McKenzie at RM 12.3; a portion of this water is diverted for cooling at an industrial containerboard processing plant and is returned to the slough; receives local and urban runoff during storm events. | 11.5 | <0.3 | Lat 44° 03′39 ″, Long 122° 58′04″ |
| HAYDEN BRIDGE/ INTAKE (mainstem) | EWEB§ treatment plant raw water intake | The intake is located immediately upstream of Hayden Bridge, which is where the most downstream USGS gauge is located. Samples collected from raw water taps within the plant itself. Includes all land uses described above. | 10.9 | 55–450 | Lat 44° 04′17 ″, Long 122° 57′48″ |

† For a map of the study site, see Supplemental Fig. S1.

‡ Flows based on 2007–2009 USGS National Water Information System data.

§ EWEB, Eugene Water and Electric Board.

River samples were collected using a combination of depth integrating techniques (Edwards and Glysson, 1999) and grab samples (Table 2). The McKenzie River and its tributaries are well mixed due to the high gradient and lack of point sources, so grab sampling was considered acceptable in lieu of unsafe alternatives. Depth integrated samples were collected in Teflon bottles using a D95 sampler, whereas grab samples were filled directly into 3-L Teflon bottles. Samples were kept on ice and in the dark, and filtered in the field within 4 h of sampling. Aliquots were subsampled using a Teflon churn splitter for filtered and unfiltered samples. Dissolved analytes were analyzed from samples filtered through precombusted 147-mm, 0.3-µm nominal pore size GF/F filters. Eugene Water and Electric Board staff collected water samples from the drinking water distribution system quarterly as part of USEPA compliance monitoring requirements for DBPs.

**Table 2. Water quality data by site and date.**

| Site† | Sample date | Sampling method‡ | DOC§¶ | POC | $A_{254}$ | Filtered THMFP | Filtered HAAFP | Unfiltered THMFP | Unfiltered HAAFP | STHMFP¶ | SHAAFP¶ | SUVA¶ | $S_{275–295}$¶ | FI¶ |
|---|---|---|---|---|---|---|---|---|---|---|---|---|---|---|
| | | | — mg $L^{-1}$ — | | $m^{-1}$ | ——— µmol $L^{-1}$ ——— | | | | – mmol THM mol $C^{-1}$ – | | L mg–$C^{-1}$ $m^{-1}$ | $nm^{-1}$ | |
| **August 2007** | | | | | | | | | | | | | | |
| MRBO | 8/16/2007 | W | 0.43 | 0.16 | 0.77 | – | – | – | – | – | – | 0.018 | – | 1.66 |
| CGRO | 8/16/2007 | W | 0.66 | <0.12 | 1.84 | 0.47 | 0.32 | 0.51 | 0.36 | 8.41 | 5.78 | 0.028 | 0.0139 | 1.52 |
| BLUE | 8/16/2007 | W | 0.64 | 0.31 | 1.97 | – | – | – | – | – | – | 0.031 | 0.0153 | 1.58 |
| Hendricks | 8/16/2007 | W | 0.75 | 0.18 | 1.65 | – | – | – | – | – | – | 0.022 | 0.0148 | 1.65 |
| Intake | 8/16/2007 | S | 0.60 | 0.18 | 1.37 | 0.39 | 0.15 | 0.42 | 0.25 | 7.76 | 3.01 | 0.023 | 0.0143 | 1.67 |
| **September 2007** | | | | | | | | | | | | | | |
| MRBO | 9/10/2007 | W | 0.31 | 0.21 | 0.67 | 0.19 | 0.07 | – | – | 7.42 | 2.77 | 0.022 | 0.0143 | 1.54 |
| CGRO | 9/10/2007 | C | 0.57 | 0.13 | 1.70 | 0.43 | 0.24 | 0.46 | 0.27 | 9.12 | 5.07 | 0.030 | 0.0154 | 1.53 |
| BLUE | 9/10/2007 | C | 0.65 | 0.37 | 2.22 | 0.52 | 0.29 | 0.65 | 0.57 | 9.54 | 5.27 | 0.034 | 0.0155 | 1.60 |
| VIDA | 9/10/2007 | W | 0.35 | <0.12 | 1.22 | 0.31 | 0.18 | – | – | 10.66 | 6.12 | 0.035 | 0.0146 | 1.50 |
| Holden | 9/10/2007 | W | 0.50 | <0.12 | 1.43 | 0.37 | 0.24 | – | – | 8.79 | 5.67 | 0.029 | 0.0147 | 1.55 |
| Camp | 9/11/2007 | C | 1.94 | 0.60 | 10.76 | 1.56 | 1.27 | 1.54 | 1.62 | 9.63 | 7.83 | 0.055 | 0.0121 | 1.59 |
| Cedar | 9/11/2007 | C | 0.90 | 0.24 | 3.14 | 0.67 | 0.61 | 0.72 | 0.55 | 8.88 | 8.15 | 0.035 | 0.0116 | 1.64 |
| Keizer | 9/11/2007 | C | 1.01 | 0.65 | 3.57 | 0.59 | 0.43 | 0.77 | 0.55 | 6.97 | 5.09 | 0.035 | 0.0116 | 1.65 |
| Intake | 9/11/2007 | S | 0.43 | 0.16 | 1.31 | 0.38 | 0.21 | 0.44 | 0.22 | 10.46 | 5.74 | 0.030 | 0.0148 | 1.62 |
| **November 2007** | | | | | | | | | | | | | | |
| MRBO | 11/16/2007 | W | 0.75 | 0.22 | 3.12 | 0.78 | 0.41 | 0.82 | 0.50 | 12.40 | 6.58 | 0.041 | 0.0132 | 1.49 |
| CGRO | 11/16/2007 | W | 1.06 | 0.27 | 3.61 | 0.90 | 0.55 | 0.92 | 0.64 | 10.19 | 6.23 | 0.034 | 0.0111 | 1.57 |
| BLUE | 11/16/2007 | W | 1.41 | 0.32 | 5.11 | 1.12 | 0.69 | 1.16 | 0.69 | 9.55 | 5.86 | 0.036 | 0.0123 | 1.52 |
| VIDA | 11/16/2007 | W | 1.22 | 0.29 | 3.63 | 0.93 | 0.68 | 0.96 | 0.54 | 9.09 | 6.71 | 0.030 | 0.0112 | 1.55 |
| Holden | 11/15/2007 | W | 1.22 | <0.12 | 3.86 | 0.91 | 0.63 | 0.97 | 0.71 | 8.90 | 6.23 | 0.032 | 0.0129 | 1.53 |
| Camp | 11/15/2007 | C | 1.88 | 0.21 | 15.03 | 1.82 | 1.66 | 1.93 | 1.74 | 11.62 | 10.62 | 0.080 | 0.0137 | 1.50 |
| Cedar | 11/15/2007 | C | 1.81 | 0.25 | 6.85 | 1.38 | 1.30 | 1.43 | 1.28 | 9.14 | 8.61 | 0.038 | 0.0128 | 1.59 |
| Keizer | 11/15/2007 | C | 1.35 | 0.26 | 4.86 | 1.03 | 0.72 | 1.12 | 0.88 | 9.15 | 6.42 | 0.036 | 0.0127 | 1.54 |
| Intake | 11/15/2007 | S | 1.20 | 0.27 | 4.28 | 1.09 | 0.55 | 1.13 | 0.64 | 10.86 | 5.50 | 0.036 | 0.0137 | 1.55 |
| **January 2008** | | | | | | | | | | | | | | |
| Intake | 1/14/2008 | S | 0.93 | | 3.70 | 0.73 | 0.37 | 0.94 | – | 9.43 | 4.83 | 0.040 | 0.0127 | 1.51 |
| **March 2008** | | | | | | | | | | | | | | |
| MRBO | 3/17/2008 | D | 0.61 | 0.13 | 1.35 | 0.38 | 0.18 | – | – | 7.43 | 3.48 | 0.022 | 0.0140 | 1.54 |
| CGRO | 3/17/2008 | D | 0.86 | 0.26 | 2.57 | 0.61 | 0.30 | – | – | 8.41 | 4.17 | 0.030 | 0.0149 | 1.49 |
| BLUE | 3/17/2008 | D | 0.91 | <0.12 | 2.64 | 0.63 | 0.36 | – | – | 8.42 | 4.75 | 0.029 | 0.0149 | 1.49 |
| VIDA | 3/17/2008 | W | 0.67 | 0.22 | 2.31 | 0.52 | 0.28 | – | – | 9.31 | 5.09 | 0.035 | 0.0138 | 1.48 |
| Holden | 3/18/2008 | W | 0.94 | 1.23 | 4.07 | 0.88 | 0.39 | – | – | 11.30 | 5.01 | 0.043 | 0.0126 | 1.47 |
| Camp | 3/18/2008 | D | 2.04 | 3.93 | 19.07 | 1.77 | 1.70 | 3.39 | 4.85 | 10.41 | 9.99 | 0.094 | 0.0128 | 1.43 |
| Cedar | 3/18/2008 | D | 1.82 | 1.08 | 20.73 | 1.87 | 1.39 | 2.39 | 2.51 | 12.37 | 9.17 | 0.114 | 0.0124 | 1.41 |
| Keizer | 3/18/2008 | D | 1.44 | 0.52 | 7.21 | 1.09 | 0.76 | – | – | 9.06 | 6.29 | 0.050 | 0.0124 | 1.52 |
| Intake | 3/18/2008 | S | 0.94 | 0.32 | 4.26 | 0.78 | 0.40 | 0.93 | 0.48 | 9.93 | 5.10 | 0.045 | 0.0119 | 1.50 |

† See Table 1 for description of sites.

‡ Letter indicates method of sample collection: D = depth integrating techniques at centroid, C = centroid grab, W = waded grab, S = raw, untreated river water sampling spigot in treatment plant.

§ DOC, dissolved organic carbon; POC, particulate organic carbon; THMFP, trihalomethane formation potential; HAAFP, haloacetic acid formation potential; STHMFP, specific trihalomethane formation potential; SHAAFP, specific haloacetic acid formation potential; SUVA, specific ultraviolet absorption; $S_{275–295}$, spectral slope; FI, fluorescence index.

¶ For graphical presentation of these data, see Supplemental Fig. S2.

Samples for DOC concentration, THMFP, and HAAFP measurements were acidified to pH 2 using reagent grade concentrated HCl immediately after filtration. Samples for DOC, THMFP, HAAFP, absorbance, and fluorescence measurements were shipped on ice within 24 h to the organic chemistry laboratory at the USGS–California Water Science Center in Sacramento, CA, and subsequently stored refrigerated at 4°C. Samples for DOC, absorbance, and fluorescence were analyzed within 5 d of collection. Samples for THMFP and HAAFP measurements were analyzed within 2 wk of collection.

Samples for POC were analyzed from filter residue. Water was passed through baked, 22-mm, 0.3-µm nominal pore size GF/F filters and the volume of filtrate noted. The filters were shipped in triplicate to the USGS–National Water Quality Laboratory in Denver, CO, and analyzed according to USEPA Method 440.0.

Dissolved organic carbon concentration was measured using high temperature catalytic oxidation with a Shimadzu TOC-V CSH TOC analyzer (Shimadzu Scientific Instruments, Columbia, MD) measuring nonpurgeable organic carbon. The mean of three to five injections was calculated for every sample and precision, described as a coefficient of variance (CV), and was <2% for the replicate injections. The absorption spectra was measured between 200 and 750 nm on filtered samples at constant temperature (25°C) with a Cary-300 spectrophotometer (Varian Inc., Palo Alto, CA) using a 10-cm quartz cell and distilled water as a blank. Specific absorbance (SUVA) was calculated by dividing absorbance at 254 nm ($A_{254}$) by DOC concentration and is reported in the units of L mg $C^{-1}$ $m^{-1}$ (Weishaar et al., 2003). SUVA values greater than 5.0 L mg $C^{-1}$ $m^{-1}$ ($n$ = 5, downstream tributaries only) were excluded from analyses because samples were presumed to contain inorganic substances with substantial absorbance at 254 nm (e.g., iron). The spectral slope parameter ($S_{275–295}$), an indicator of DOM composition, was calculated using a nonlinear fit of an exponential function to the absorption spectrum over the wavelength range 275 to 295 nm as described by Twardowski et al. (2004). Low concentration samples that fit the regression equation poorly ($R^2$ < 0.95) were excluded from subsequent analyses.

Fluorescence EEMs were measured on filtered samples with a SPEX Fluoromax–4 spectrofluorometer (Horiba Jobin Yvon, Edison, NJ) using a 150W Xenon lamp, a 5-nm band pass, and 0.050-s integration time. Fluorescence intensity was measured at excitation wavelengths of 200 to 440 nm at 10-nm intervals and emission wavelengths of 220 to 600 at 5-nm intervals on room temperature samples (25°C) in a 1-cm quartz cell. Lamp and water-Raman checks were performed daily per the manufacturer's specifications. EEMs were blank corrected in MATLAB 7.7.0 (Mathworks, Inc., Cambridge, MA) to remove Raman scattering and normalized to the daily Raman peak area. Rayleigh scatter lines were removed after blank correction (Stedmon et al., 2003). Instrument bias was corrected using manufacturer's supplied excitation and emission correction factors. Inner filter corrections were applied to EEMs with $A_{254}$ greater than 0.03 (1-cm cuvette) as described by McDonald (1997). The Fluorescence Index (FI), used to indicate DOM contributions from algal vs. terrestrial sources, was calculated as a ratio of emission intensities at 470 nm to 520 nm and an excitation wavelength of 370 nm (McKnight et al., 2001; Jaffe et al., 2008).

Disinfection byproducts formation potential (DBPFP) was determined on both filtered and unfiltered samples to determine the relative importance of the dissolved and particulate OM fractions. Both THMFP and HAAFP were determined following a modified version of USEPA Methods 502.2, 510.1, and 552.2 as described by Crepeau et al. (2004). The method involved a 7-d reaction time, pH buffered at 8.3, temperature held at 25°C, and final, residual-free chlorine concentration restricted to 2 to 4 mg $L^{-1}$. Chlorine dosing and quenching was done at the USGS Lab, Sacramento, CA, as were analyses for THM concentrations. Determination of HAAs was done by Truesdail Laboratories, Inc., Tustin, CA. THMFP included measurement of all four THM species ($Cl_3CH$, $Br_3CH$, $ClBr_2CH$, and $Cl_2BrCH$), whereas HAAFP included five HAA species (ClAA, $Cl_2AA$, $Cl_3AA$, BrAA, and $Br_2AA$, where AA denotes acetic acid). We reported DBP concentration data as µmol-DBP $L^{-1}$ to account for molecular weight differences among the various THM and HAA species. Specific trihalomethane formation potential (STHMFP) and specific haloacetic acid formation potential (SHAAFP) were calculated by dividing molar DBPFPs by DOC concentration and are reported as mmol–DBP mol $C^{-1}$.

In addition to analyses of collected water samples, treatment plant and distribution system data were provided by EWEB including TOC data for samples collected at the treatment plant intake (i.e., raw water) and at the point of entry to the distribution system after coagulation, chlorination, and filtration (i.e., finished water). THM and HAA concentration data reported from EWEB's distribution system were determined following USEPA Method 551.1 and SM6251B, respectively.

Discharge data were obtained from the USGS National Water Information System (http://waterdata.usgs.gov). Of the 10 sites sampled, three were ungaged and the remaining were gaged by USGS. Discharge at Camp Creek was estimated—based on comparisons with the nearby Mohawk River and Cedar Creek discharges. Both were gaged for previous dates when Camp Creek flow was measured directly by EWEB. Discharge in Keizer Slough was estimated from previous measurements by EWEB. The variability in flows at Keizer Slough is low—resulting in relatively straightforward estimates.

## Statistical Analysis

To determine significant differences across site and date, analysis of variance was run with site and date as the main effect, followed by Fisher's least significant difference posthoc test. Differences were considered significant when P values were <0.05. Simple and multiple regression analyses were used to examine relationships among parameters. Parallel Factor Analysis (PARAFAC), a multivariate statistical modeling approach used to decompose the full EEM's signal into underlying individual fluorescent components, was run on EEMs data using the N-way Toolbox version 3.10 (Anderson and Bro, 2000; http://www.models.life.ku.dk/source/nwaytoolbox) for excitation 240 to 600 nm and emissions 290 to 600 nm after removal of the water Raman region as described by Stedmon and Bro (2008). Several PARAFAC models were run to identify the number of components that resulted in the lowest possible residuals but yet contained spectral properties relevant to fluorophores found in the literature. The PARAFAC model goodness of fit was determined

by verifying that the percent difference between the measured and modeled excitation/emission (ex/em) pairs was low (<10%), as well as by overall low residual intensities (<0.01) characterized by noise, and good agreement between duplicates (Cory and McKnight, 2005; Jaffe et al., 2008). Principal component analysis (PCA), commonly used on multiparameter datasets to reduce the number of variables and detect structure in the data, was run on the PARAFAC components to determine if these parameters could distinguish DOM derived from different sources. Regressions, PCA, and partial least square regression analyses were run using Unscrambler version 9.2 (Unscrambler, 2005). All other statistical analyses were conducted with SYSTAT, version 8.0 (SPSS Inc., 1998).

## Results and Discussion

### Dissolved Organic Carbon, Particulate Organic Carbon, and Total Organic Carbon Concentrations

Dissolved organic carbon concentrations for samples collected in this study ranged between 0.3 and 2.0 mg $L^{-1}$ (Table 2). Concentrations were significantly higher in November and March compared to August and September, which may reflect high flow events. The first two sampling campaigns in August and September were conducted during base flows of about 53 $m^3$ $s^{-1}$ at the intake, whereas the three subsequent samplings took place during significant storm events during peak mainstem flows that exceeded 300 $m^3$ $s^{-1}$ (Fig. 2; Supplemental Fig. S3). For all sampling dates, concentrations were lowest at the upstream site McKenzie River above the South Fork (MRBO) and highest at the three lower tributary inputs. Concentrations of DOC in water flowing out of the two reservoirs were significantly greater than the MRBO site—by 0.2 to 0.7 mg $L^{-1}$, resulting in a 10 to 60% increase in mainstem DOC concentrations relative to MRBO.

In general, there was little change in DOC concentration between the mainstem sites downstream from the reservoirs, indicating that both tributary inputs and riverine processing had little effect on mainstem DOC loads along the lower stretch of the river. In November, concentrations were higher at Holden and the intake (0.94 mg $L^{-1}$) compared to the upstream site VIDA (mainstem site located downstream of the two reservoir inflows), which was 0.67 mg $L^{-1}$. However, this increase can be attributed to runoff inputs resulting from the intense rainfall event occurring overnight and during the second day of sampling, which confounded comparison of upstream and downstream concentrations. With the exception of several of the tributary samples, especially during the March storm event, POC concentrations were generally <0.3 mg $L^{-1}$ and represented less than one-third of the TOC pool (Table 2).

Between 2004 and 2009, EWEB's reported TOC concentrations in raw water entering the treatment plant were typically <2 mg $L^{-1}$, averaging 0.9 ± 0.3 mg $L^{-1}$ (Supplemental Fig. S4). Trends from EWEB sampling and our study showed a strong relationship between EWEB's raw water TOC and the combined DOC and POC data obtained from this study ($R^2$ = 0.81, $n$ = 4; Fig. 1). However, TOC concentrations calculated from the USGS data as the sum of DOC and POC were notably higher (30–50%) on most dates compared to EWEB's TOC values. This agrees with previous work that showed oxidation of unfiltered samples frequently underestimated the TOC pool (Aiken et al., 2002). Likely reasons for this include incomplete conversion of particulate C to $CO_2$, the settling out of particles before analysis, and/or lengthy holding times during which biological transformations can occur.

Examination of EWEB's multiyear data revealed that the first major storm events of the fall, typically occurring in November, are associated with elevated raw water TOC concentrations (Fig. 1). Subsequent storm events are also associated with higher than average TOC concentrations. Increases in both DOC and POC concentrations during storm events are commonly reported and reflect a shift from groundwater flow paths to overland flow and passage through organic-rich surface soils (e.g., McGlynn and McDonnell, 2003; Dalzell et al., 2005; Vidon et al., 2008). Particularly high DOC concentra-

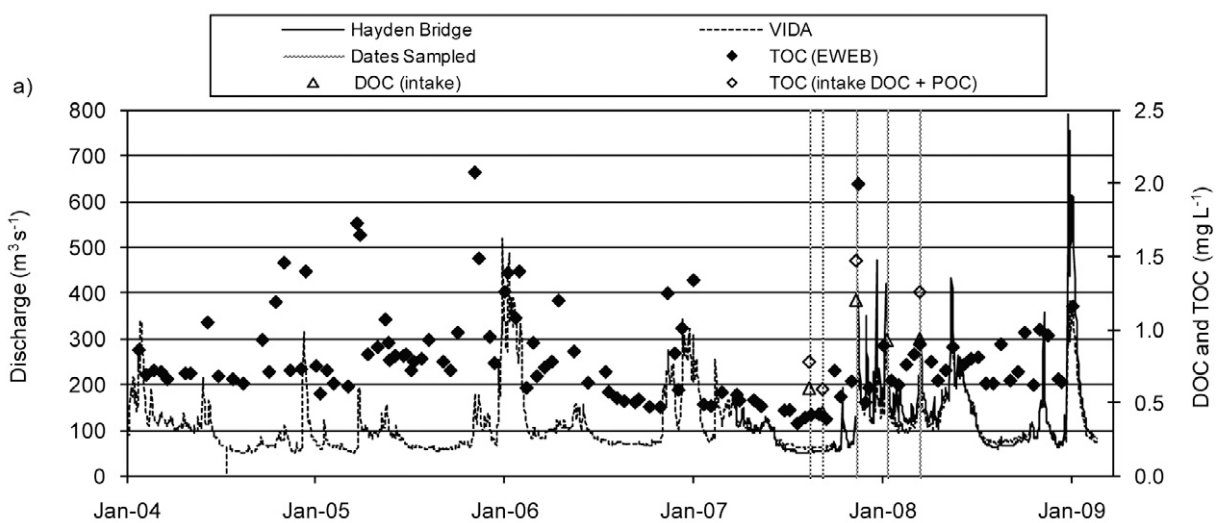


**Fig. 1. Discharge and organic carbon concentrations in the McKenzie River from 2004–2009. Solid and dashed lines indicate discharge for the McKenzie River at Hayden Bridge and VIDA, respectively. Vertical dotted lines indicate sampling dates for this study. Filled diamonds represent Eugene Water and Electric Board's reported raw water total organic carbon concentrations (TOC). Open triangles represent dissolved organic carbon (DOC) and open diamonds represent TOC calculated as the sum of dissolved and particulate carbon (DOC + POC) measured at the intake during this study. For details of the study period, see Supplemental Fig. S3.**

tions are often associated with the first storm events of the rainy season when flushing of surface soils mobilizes DOC that has accumulated in the soil profile (Boyer et al., 1997; Sanderman et al., 2009). Higher terrestrial DOC inputs may also be derived from the leaching of newly deposited litter material, particularly following fall leaf loss (Hinton et al., 1997; Schiff et al., 1997; Stepczuck et al., 1998; Chow et al., 2009).

## Watershed Trihalomethane and Haloacetic Acid Precursors

Laboratory formation potentials for THMs and HAAs measure the amount of DBPs that form under the specified chlorination conditions. Because the contact time used in this study was 7 d, the amount of THMs and HAAs formed are greater than would be expected under EWEB's typical drinking water treatment processes. Furthermore, these samples did not undergo coagulation and filtration treatment, as does all water that passes through EWEB's drinking water treatment plant. Rather than being indicative of absolute amounts of DBPs that may form within a distribution system, formation potentials provide information about raw water DBP precursor concentrations. Thus, we focused on relative differences among samples.

There was a wide range in both THMFP (0.19–1.87 μmol $L^{-1}$; 27–240 μg $L^{-1}$) and HAAFP (0.07–1.67 μmol $L^{-1}$; 10–250 μg $L^{-1}$) (Table 2). The majority of DBPs that formed were chlorinated species. Chloroform accounted for 78 ± 10% of the total THM pool and dichloro plus trichloro acetic acids accounted for 96 ± 3% of the total HAA pool. There was a strong correlation between DOC concentration and both THMFP ($R^2$ = 0.94, $n$ = 36) and HAAFP ($R^2$ = 0.90, $n$ = 36), indicating that DOC concentration was the major driver of DBPFP. Because of this, trends in DBPFP by site and date closely followed those discussed earlier for DOC concentration.

Because EWEB chlorinates its drinking water before filtration, with a chlorine contact time of 2 to 12 h before filtration is completed, particulates could be important in the formation of DBPs. Comparison between the filtered and unfiltered samples indicated that on average 11 and 19% of unfiltered water THMFP and HAAFP, respectively, can be attributed to POC (Table 2). Excluding the two tributary sites sampled in March, which had high POC contributions, there was a strong correlation between filtered and unfiltered samples for both THMFP ($R^2$ = 0.98, $n$ = 19) and HAAFP ($R^2$ = 0.93, $n$ = 18). This suggests that in this system DBP precursors are predominantly in the dissolved fraction and filtered water samples are good predictors of unfiltered water DBPFP.

Measured THM and HAA concentrations of DBPs, particularly HAAs, from within EWEB's distribution system were elevated between 2005 and 2007 but in 2008 appeared to return to concentrations comparable to prior years (Supplemental Fig. S4). This period of elevated concentrations coincided with the refilling of Cougar Reservoir following the drawdown period to modify the withdrawal structure (Anderson, 2007). Hypothesized effects of the reservoir drawdown and construction project that may have increased downstream DBP precursor concentrations included (i) release of OM from oxidized sediments and/or decomposing vegetation that grew on the exposed bed material during the drawdown period that was inundated when the reservoir was refilled, and/or (ii) increases in DOM inputs from reservoir planktonic algal production in epilimnetic (10 to 20 m) water that was released to meet downstream temperature criteria. However, this period also coincided with several changes in treatment plant operations, including switching from lime to caustic soda for pH adjustment, changing temporarily from an alum coagulant to a polyaluminum chloride (PACl) coagulant, and ceasing a superchlorination/dechlorination process (HDR Engineering, 2007). For these reasons, available data were not sufficient to establish whether changes in source water quality and/or treatment plant operations were responsible for the measured increases in DBPs.

Because there is a limited amount of DBP concentration data, and because the distribution system samples were not always collected in concert with the samples collected for this study, we cannot compare the 2007 and 2008 laboratory formation potential results to the THM and HAA concentrations measured within the distribution system. Similarly, because the raw water TOC data were collected on a different schedule than the distribution system DBP data, and because there were notable changes in TOC concentration, THMFP and HAAFP over short timescales, we were unable to determine whether a relationship exists between TOC concentrations (both in raw and finished water) and DBP concentrations within the distribution system. It is also unclear, based on available EWEB data, whether TOC concentrations were greater between 2005 and 2007 when distribution system DBPs were elevated (Supplemental Fig. S4).

## Dissolved Organic Matter Reactivity: STHMFP and SHAAFP

Normalizing THMFP and HAAFP by DOC concentration to obtain STHMFP and SHAAFP, respectively, provides an indication of how reactive the DOC pool is on a molar basis. Seasonal trends suggest that in addition to containing higher concentrations of DOC and POC, the first storm event in the fall contributed DOM that has a higher propensity to form DBPs. Both STHMFP and SHAAFP were highly variable, ranging from 7 to 12 mmol THM mol $C^{-1}$ and 3 to 10 mmol HAA mol $C^{-1}$, respectively (Table 2). The upstream mainstem site (MRBO) had notably lower STHMFP and SHAAFP in August and March compared to other sites. However, reactivity during the first storm event of the season (November) was much higher, possibly explained by the leaching of plant and soil material high in aromatic content from the highly forested upper basin during this first flush event of the season (see below).

The lower tributary creeks, Camp and Cedar, had significantly higher SHAAFP compared to all other sites. However, STHMFP was not consistently high for these sites. In contrast to these two tributary creeks, Keizer Slough did not have notably high SHAAFP despite having elevated DOC concentrations. Keizer Slough receives most of its water from the McKenzie River upstream at RM 16 rather than from local watershed sources like Camp and Cedar creeks. Additional water enters the slough from local urban runoff and passes by a wood products manufacturing plant, where it is used as cooling water but receives no effluent. The lack of high HAA precursor content in Keizer Slough DOM suggests that HAA precursors in Camp and Cedar creeks are largely derived from upstream terrestrial sources, particularly drainage of forested and agri-

cultural lands. Research suggests that HAA precursors have a higher aromatic content than THM precursors (Croué et al., 2000, Liang and Singer, 2003) and HAA precursors have been associated with terrestrially derived fulvic and humic acids characterized by high aromatic content (Kraus et al., 2008).

Dissolved organic matter exiting both of the reservoirs was generally intermediate in both STHMFP and SHAAFP. This is not surprising since upstream variability in DOM composition is moderated by reservoir storage capacity and residence time. For example, pulses of high DBP forming material that may enter the reservoir during winter storm events are likely to be mixed with less reactive material already in the reservoir—before downstream release. In-reservoir processes such as algal production and degradation of bottom sediments can increase DBP precursor concentrations, whereas biodegradation and photodegradation may lead to their loss or transformation (Aiken and Cotsaris, 1995; Downing et al., 2008). During this study, there was no indication that water exiting the Cougar Reservoir was high in DBP precursor content despite evidence from the treatment plant (HDR Engineering, 2007) and EWEB's ambient monitoring program (Morgenstern et al., unpublished data). This suggests that if the Cougar Reservoir drawdown, construction, and refilling contributed to higher DBPs from 2005 to 2007, these effects had apparently abated before this study.

There was a significant but poor correlation between STHMFP and SHAAFP ($R^2$ = 0.33, $n$ = 30), indicating that precursor sources for these two classes of DBPs differ. This has been found in several previous studies (Krasner et al., 2006; Hua and Reckhow, 2007; Kraus et al., 2008) and arises because reaction pathways differ for the formation of these two different classes of DBPs (Reckhow et al., 1990; Liang and Singer, 2003). This lack of correlation highlights the need to examine the sources, transport, and fate of different classes of DBP precursors.

## Optical Proxies for Dissolved Organic Carbon Concentrations

The use of optical properties as proxies for DOC concentration has been recognized for many years in the field of oceanography (Coble, 2007). Recently, several studies have shown that absorption coefficients (e.g., $A_{254}$, $A_{330}$, and $A_{440}$) and fluorescence at excitation 370 nm and emission 460 nm, defined here as fluorescent dissolved organic matter (FDOM), are good predictors of DOC concentration in surface waters (e.g., Bergamaschi et al., 2005; Belzile et al., 2006; Downing et al., 2009; Saraceno et al., 2009). In this dataset, fluorescence was a better predictor of DOC concentration than $A_{254}$ (Table 3). The weaker relationship between $A_{254}$ and DOC concentration ($R^2$ = 0.73 vs. 0.92 for FDOM, $n$ = 33) largely resulted from several of the downstream tributary samples that had high $A_{254}$ values relative to DOC concentration (Supplemental Fig. S5). Closer inspection of the absorbance curves suggests that there may be interference due to the presence of ferric iron in these samples (Weishaar et al., 2003). Another potential interference can arise from colloids, which are not removed by filtration (Hudson et al., 2007). When the lower stream tributaries were not included in the analysis there was a stronger correlation between $A_{254}$ and DOC ($R^2$ = 0.86, $n$ = 24).

There was a strong correlation ($R^2$ > 0.90) between DOC concentration and several fluorescence excitation-emission pairs including FDOM (Fig. 2). The strongest prediction ($R^2$ = 0.93, $n$ = 33) was derived from the EEMs region falling within excitation 320 to 370 nm and emission 420 to 475 nm. This region includes the commonly measured FDOM (excitation 370 nm, emission 460 nm) and peak C fluorophores, which are associated with terrestrial-derived humic and fulvic-like material (Coble, 2007). A partial least squares regression using all 904 EEMs fluorophores provided even better predictive ability ($R^2$ = 0.96, $n$ = 30) for DOC than the individual fluorophores.

## Optical Properties as Proxies for THMFP and HAAFP

While $A_{254}$ was significantly correlated to both THMFP and HAAFP ($R^2$ = 0.84 and 0.85, respectively, $n$ = 30), there was again a stronger relationship ($R^2$ > 0.90) between the fluores-

**Table 3. $R^2$ values for various predictors of dissolved organic carbon (DOC) concentration, trihalomethane formation potential (THMFP), and haloacetic acid formation potential (HAAFP).**

| Predictor | DOC $n$ = 33 | THMFP $n$ = 30 | HAAFP $n$ = 30 |
|---|---|---|---|
| | mg L$^{-1}$ | μmol THM L$^{-1}$ | μmol HAA L$^{-1}$ |
| DOC concentration | – | 0.94 | 0.90 |
| UV–254 | 0.73 | 0.84 | 0.84 |
| Individual fluorophores† | 0.93 | 0.96 | 0.93 |
| FDOM (ex. 370/em. 460) ‡ | 0.92 | 0.95 | 0.92 |
| Entire EEM spectra (PLS)‡ | 0.96 | 0.97 | 0.95 |
| PARAFAC component 1‡ | 0.44 | 0.55 | 0.57 |
| PARAFAC component 2 | 0.93 | 0.95 | 0.91 |
| PARAFAC component 3 | 0.11 | 0.11 | 0.13 |
| PARAFAC component 4 | 0.66 | 0.62 | 0.67 |
| PARAFAC components 1–4 (PLS) | 0.98 | 0.98 | 0.96 |

† $R^2$ values listed here are highest values found among all 904 excitation–emission pairs. See Fig. 2 for the full range of values.

‡ FDOM: fluorescent dissolved organic matter; PLS: partial least squares regression. EEM: excitation-emission matrix. PARAFAC: parallel factor analysis.

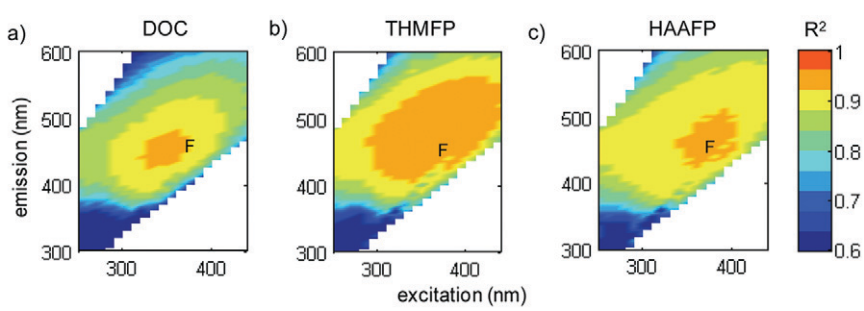


**Fig. 2. $R^2$ values for Pearson's correlation between individual excitation-emission matrix fluorophores and (a) dissolved organic carbon (DOC) concentration, (b) trihalomethane formation potential (THMFP), and (c) haloacetic acid formation potential (HAAFP). The letter "F" indicates the location of the commonly measured fluorescent dissolved organic matter (FDOM) fluorophore (exitation 370 nm, emission 460 nm).**

cence data and both THMFP and HAAFP (Table 3, Fig. 2). In fact, some of the fluorescence data showed a better relationship with THMFP and HAAFP than with DOC concentration.

Historically, $A_{254}$ has been proposed as a good proxy for DOC concentration and THMFP (Edzwald et al., 1985). However, Weishaar et al. (2003) pointed out that the slope of the $A_{254}$–DOC relationship can vary. This suggests that in systems where DOM composition differs, changes in the absorbing pool may not be coupled to changes in the bulk DOC nor DBP precursor pool. In addition, a strong relationship between $A_{254}$ and THMFP was believed to exist because absorbance at 254 nm per unit of C has been shown to reflect aromatic C content (Weishaar et al., 2003) and the aromatic C pool has been associated with the formation of THMs (Reckhow et al., 1990; Croué et al., 1999; Singer, 1999; Wu et al., 2000). However, several studies have shown that nonaromatic, non-UV absorbing moieties can make up a significant portion of the DBP precursor pool, particularly for THMs (Reckhow et al., 1990; Liang and Singer, 2003; Kraus et al., 2008). It is likely that strong correlations between $A_{254}$ and THMFP exist in instances when both of these parameters are strongly linked to bulk DOC concentration. Another potential interference can arise from constituents such as iron, nitrate, and colloids, which also absorb around $A_{254}$ (Weishaar et al., 2003; Hudson et al., 2007). In this dataset, we believe interference from iron and/or colloids compromised the absorbance data for several of the downstream tributaries, which were sampled during storm events that mobilized significant amounts of particulate material (Supplemental Fig. S5).

A subset of DOM that absorbs light energy will fluoresce. Thus, fluorescence is also associated with aromatic moieties (McKnight et al., 2001; Cory and McKnight, 2005). However, because most common inorganic species that absorb light do not fluoresce, there may be less interference in this measurement than with absorbance spectroscopy. In addition, fluorescence can discriminate between different sources of chromophoric DOM that absorb at similar wavelengths but fluoresce at different ones (Stedmon et al., 2003; Henderson et al., 2009). As was noted for DOC concentration, the commonly used FDOM pair proved to be a good predictor of both THMFP and HAAFP for these samples, with $R^2$ values of 0.95 and 0.92, respectively (Table 3). However, slightly longer wavelengths provided the best predictive ability for both THMFP and HAAFP. For THMFP, $R^2$ values of 0.96 were found for fluorescence pairs with excitations of about 370 to 390 nm and emissions of 460 to 500 nm, whereas HAAFP $R^2$ values of 0.93 were found for fluorescence pairs with excitations of about 380 to 400 nm and emissions of 450 to 480 nm (Fig. 2). A shift to longer wavelengths has been shown to be associated with terrestrial DOM with high aromatic content (McKnight et al., 2001; Hood and McKnight, 2003). This region is also closer to peak D (excitation 390 nm and emission 510 nm) associated with soil fulvic acids (Stedmon et al., 2003). Previous work has suggested that DOM derived from soil and degrading plants has higher propensity to form HAAs compared to fresh plant and algal sources, which have lower aromatic content (Kraus et al., 2008).

Interestingly, a larger number of fluorescence pairs were strong predictors ($R^2 > 0.90$) for THMFP and HAAFP than for DOC concentration (Fig. 2). This is probably because like THMFP and HAAFP, fluorescence is determined by both the concentration and composition of DOM. Therefore, this illustrates that, in this system, there is a large overlap of DOM moieties, which are both chromophoric and react with chlorine to form DBPs. Similarly, Nakajima et al. (2002) found that THM precursors contributed to fluorescence to a larger degree than non-THM forming DOM. As was seen with DOC concentration, a partial least squares regression using all 904 excitation-emission pairs provided even better predictive ability for both THMFP ($R^2 = 0.98$, $n = 30$) and HAAFP ($R^2 = 0.96$, $n = 30$) than individual fluorescence pairs (Table 3). This result supports the idea that there are a variety of organic compounds with different chemical moieties in the DBP precursor pool.

## Optical Properties Indicative of Dissolved Organic Matter Composition

Because the interaction of a filtered water sample with light is determined both by DOM amount and composition, the additional benefit to measuring optical properties of DOM is that it provides qualitative information about the DOM pool. For absorbance data, in addition to SUVA being used as a proxy for aromatic content, spectral slope ($S_{275–295}$) of the absorbance curve has been shown to relate to DOM aromatic content and molecular weight; decreasing $S_{275–295}$ is associated with higher aromatic content and increasing molecular weight (Helms et al., 2008; Spencer et al., 2009). Similarly, fluorescence data have been shown to provide information about DOM character and origin. FI has been widely used to indicate relative contributions of algal vs. terrestrial-derived DOM. Higher FIs are associated with algal-derived material, which has lower aromatic content and lower molecular weight, whereas lower FI values are associated with more highly processed, terrestrial-derived material, which has greater aromatic content and higher molecular weight (McKnight et al., 2001; Jaffe et al., 2008). Qualitative information can be derived from the identification of peaks in the EEMs spectra reflective of different DOM pools such as humic and fulvic acids, protein-like material, and phytoplankton-derived material (Stedmon et al., 2003; Coble, 2007; Hudson et al., 2007; Fig. 3). The application of PARAFAC is used to identify different classes of OM, which make up the entire EEMs spectra. The relative proportions of these components can reveal both quantitative and qualitative differences between samples (Jaffe et al., 2008; Stedmon and Bro, 2008; Cook et al., 2009).

### SUVA, $S_{275–295}$, FI

In November, the DOM entering the McKenzie River from the upstream site MRBO had a notably high SUVA, low FI, and low $S_{275–295}$ values, indicative of terrestrial-derived DOM mobilized from shallow surface soils and the forest floor (Table 2; Supplemental Fig. S2). The November sampling took place during the first major storm event of the season when DOM mobilized from these shallow surface soils would be expected to contain higher concentrations of aromatic, high molecular weight DOM, similar to signals reported for spring snowmelt events (Neff et al., 2006; Spencer et al., 2008; Sanderman et al., 2009). An increase in highly aromatic material, including lignin and other phenols, likely explains the high STHMFP and SHAAFP of this sample (Table 2).

Together, the qualitative parameters gave no indication that there was a significant contribution of algal-derived DOM in either of the reservoirs. Algal-derived material is associated with a higher FI, lower SUVA, and higher $S_{275–295}$ values, and contributions of algal-derived material are expected to be greatest in the summer and fall. If anything, SUVA values were higher and FI values lower in reservoir outflows compared to the mainstem sites (Table 2). While $S_{275–295}$ values were greater below the reservoirs compared to other sites, high S values have also been associated with photobleaching (Helms et al., 2008). The two reservoirs showed the least amount of change in both FI and SUVA values by date, which again probably reflects buffering of the DOM pool due to reservoir storage capacity and longer residence times. The sites below Blue River Reservoir and Cougar Reservoir had strikingly similar FI, SUVA, and S values for each sampling date, suggesting sources and processing of DOM in these two reservoirs are similar. Although these data do not rule out the possibility that bottom sediments that formed during the drawdown of Cougar Reservoir contributed DOC and DBP precursors to Cougar Reservoir after it was refilled in 2005, there was no indication that DOM sources to Cougar Reservoir differed from Blue River Reservoir during the study period.

For the mainstem and tributary sites, August and September samples generally had lower SUVA, higher FI, and higher $S_{275–295}$ values compared to the December, January, and March samples. This indicates a shift toward high molecular weight and terrestrial-derived materials during periods of greater surface water runoff. FI values were particularly low for Camp and Cedar creeks during the peak runoff event sampled in March. Higher FI, higher $S_{275–295}$, and lower SUVA values in the mainstem and tributary samples during the summer and fall months may also be attributable to DOM derived from sloughed periphyton (Perry and Perry, 1991).

Fluorescence properties have also been used to identify wastewater sources of DOM. An increase in protein-like peaks T and B is associated with sewage-derived material, presumably due to the production of DOM from microbial activity (Baker et al., 2003; Hudson et al., 2007; Henderson et al., 2009). In March, there was a prominent signal in this region for the two uppermost mainstem sites, MRBO, and VIDA (data not shown). This may reflect DOM contributions from local septic systems, which become saturated during storm events. The higher FI values at MRBO in March relative to other sites may also reflect the microbial signal arising from leaking septic systems (Jaffe et al., 2008). The Eugene Water and Electric Board has conducted some limited investigations on the water quality impacts to the McKenzie River from higher densities of septic systems located near the river in gravelly soils. Preliminary results suggest slight increases in bacteria and nutrients are associated with septic cluster areas (Morgenstern et al., 2009). Both MRBO and VIDA are located downstream from several of these septic cluster areas.

## Parallel Factor Analysis of EEMs Spectra

The application of a four-component PARAFAC Model to the EEMs data provided good agreement between measured and modeled EEMs spectra (Supplemental Fig. S6), and the four

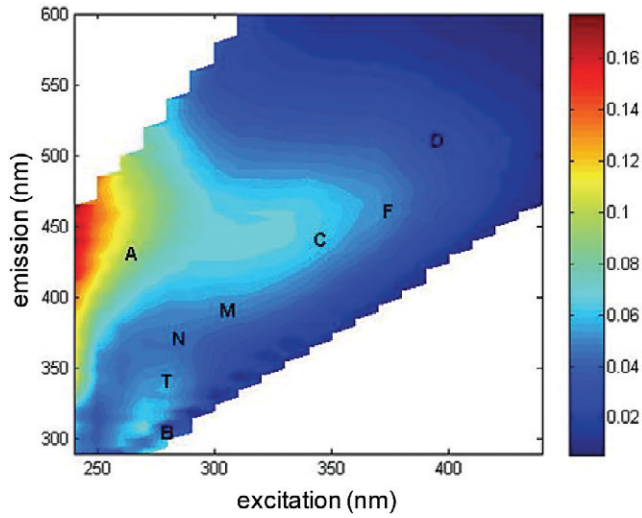


**Fig. 3. Example of a typical corrected excitation-emission matrix (EEM) plot. Data shown are from the March intake sample. The letter F shows the location of the fluorescent dissolved organic matter (FDOM) pair at excitation 370 emission 460, and other letters indicate previously identified fluorophores (Stedmon et al., 2003; Coble, 2007).**

modeled components represent peaks that have been previously identified as associated with different DOM pools (Table 4; Stedmon et al., 2003; Coble, 2007; Hudson et al., 2007; Cory and McKnight, 2005). Component 1 (C1) encompassed peak A and has been associated with terrestrial-derived fulvic and humic acids, whereas component 2 (C2) included peak A and peak C, which is also associated with terrestrial-derived DOM. Component 3 (C3) was specific to lower emissions (305 nm) centered on an excitation maxima of 270 nm, which is commonly identified by peak B associated with protein-like material. Component 4, although less distinct than the other components and responsible for <15% of the total component loadings for individual samples, had a peak centered at the EEMs region identified by protein-like peak T (ex/em 270/340 nm) and also encompassed the regions N and M, which have been associated with phytoplankton productivity and "marine-like" humics.

Regression analyses among the four different PARAFAC components and DOC concentration, THMFP, and HAAFP indicate that C2 has by far the strongest relationship with these parameters (Table 3). This is not surprising since fulvic and humic acids, which are associated with peaks A and C, are known to contain the bulk of aqueous DOM and contain aromatic moieties that are known DBP precursors (Liang and Singer, 2003). The poor correlation between C3 and these parameters

**Table 4. Positions of the fluorescence maxima of the 4 components identified by the Parallel Factor Analysis (PARAFAC) Model.**

| Component no. | Excitation max. | Emission max. | Previously identified peaks and associations† |
|---|---|---|---|
| | —— nm —— | | |
| C1 | 250 | 380–460 | A: humic-like; second order Rayleigh scattering |
| C2 | 250 & 360 | 460 | A & C: humic-like |
| C3 | 270 | 305 | B: protein-like material |
| C4 | 280–330 | 340–380 | T: protein-like; M & N: marine humic-like, phytoplankton productivity |

† For details on previously identified peaks see Stedmon et al. (2003); Stedmon and Markager (2005); Coble (2007); Hudson et al. (2007). Graphs of the 4 PARAFAC components are shown in Supplemental Fig. S7.

suggests that the portion of the DOM pool associated with fresh, protein-like material is not strongly linked to bulk DOC concentration nor to the pool of DOC that forms THMs and HAAs.

We applied PCA to the four EEM PARAFAC components as well as to the FI to examine whether the fluorescence data revealed changes in DOM composition by site and date (Fig. 4). The results of the PCA explained 71% of the variability in the dataset (43% for PC1 and 28% for PC2). The proximity of the August and September data relative to November and March in the PCA scores plot indicates a shift in DOM composition by date. In August and September, samples were associated with higher FI and PC4, suggesting that during this period McKenzie River DOM contains more of an algal source. The November samples contained greater amounts of C2 and lower amounts of C1 compared to the March samples. Since C2 appears to be more linked to DBPFP than C1, this agrees with the finding that the November samples had higher DBP precursor content. This supports the idea that C2 is associated with DOM mobilized from litter material and shallow soil layers during early winter storm events. This pool of DOM is more likely to contain high concentrations of aromatic, high molecular weight, lignin-like material (Hood et al., 2006; Hernes et al., 2008; Spencer et al., 2008; Vidon et al., 2008; Sanderman et al., 2009).

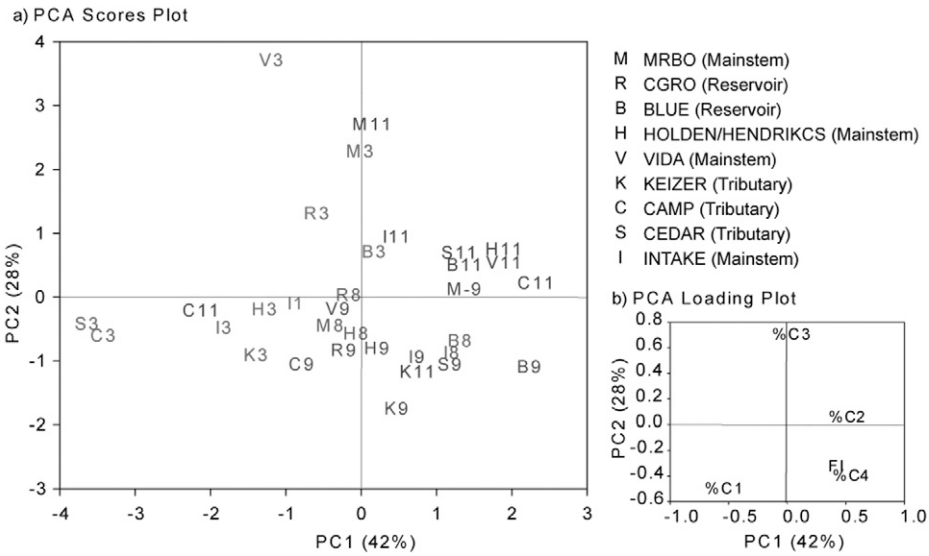


**Fig. 4. Results of the principal component analysis (PCA) of the excitation-emission matrix (EEM) PARAFAC data and the fluorescence index including the (a) scores plot and (b) loading plot. In the scores plot, letters indicate sites and numbers associated with sites indicate sampling month (e.g., 3 = March). Loading plots show percent parallel factor analysis (PARAFAC) component loadings (C1 to C4) and fluorescence index (FI).**

The presence of peak B fluorescence associated with PARAFAC C3 distinguished the March MRBO and VIDA sites. As discussed previously, this signal may reflect the addition of DOM from local septic systems, which were inundated due to a rise in the water table during the March storm event. There was also a potential signal from these systems in the November MRBO site, although leaching of fresh plant material during the first storm of the season could also contribute to higher protein-like fluorescence.

It is noteworthy that DOM from the sites below the two reservoirs was not clearly distinguishable from other sites. In August and September, DOM below the Blue River Reservoir showed a shift toward higher FI and PARAFAC C4, suggesting that algal inputs during the summer months may have had a notable effect on DOM composition in this reservoir. The March samples for both reservoirs shifted more toward the March upstream site MRBO, which supports the idea that inflow sources to these reservoirs are similar to MRBO. However, the reservoir sites generally fell toward the center of the PCA scores plot, indicating that they contain a mixture of DOM sources. Again, reservoir storage capacity and longer residence time is expected to attenuate any signal coming from algal blooms or changes in inflow DOM source and composition.

In March, DOM from the two downstream tributaries Camp and Cedar creeks was clearly distinguishable from the other samples due to high PC1 scores. These samples had high loadings for PARAFAC C1 but low loadings for the other fluorescence parameters. An increase in the C1 associated with peak A without a similar increase in peak C represented by C2 suggests DOM contributing to these fluorescence regions are not necessarily linked, even though both have been associated with humic material derived from terrestrial sources (Coble, 2007).

## Conclusions and Implications

Results from this study showed that watershed DOM inputs to the McKenzie River originate primarily from upstream terrestrial inputs. Our data indicate that seasonal changes in DOM amount and composition are linked to changes in hydrologic flow path. During the summer and fall when upstream sources come primarily from groundwater flow, DOC concentrations are low (<0.5 mg $L^{-1}$). With the onset of winter rains and saturated soil conditions, the hydrologic flow path shifts to shallow surface soils and surface runoff, which mobilizes a higher molecular weight, aromatic-rich DOC pool. In particular, the first major rain event of the season appears to transport DOC that is rich in DBP precursors.

Although the downstream tributaries contained significantly higher concentrations of DOC, which had high HAA precursor content, these tributaries contributed <5% of the total flow in the mainstem. Under current conditions, precursor loads from these sources have minimal effect on drinking water quality. Reservoir outflows had higher DOC concentrations than the upper watershed site represented by MRBO. However, qualitative data do not indicate a significant contribution from in situ algal production. Instead, elevated reservoir concentrations may reflect the inflow of high DOC containing water during winter months that is then released over time.

DOC concentration and composition were similar for both of the reservoirs, providing no indication that the 2002–2004 drawdown and subsequent refilling of the Cougar Reservoir affected DBP precursor concentrations during the study period. However, because watershed DOC data are not available for

2004–2006 when higher DBPs were measured in EWEB's distribution system, we cannot rule out the effects of the drawdown during the period immediately following reservoir refilling.

Fluorescence data provided a better proxy for both THMFP and HAAFP than either DOC concentration or $A_{254}$ (Table 3). The strongest prediction of these parameters was found using multiple linear regression of the four modeled PARAFAC components. $R^2$ values were 0.98 and 0.96 for THMFP and HAAFP, respectively. However, individual fluorescence pairs also provided very good predictive ability for DBPs. THMFP was best predicted by ex/em of about 380/480 nm with an $R^2$ of 0.96, whereas HAAFP was best predicted by ex/em of about 390/460 nm with an $R^2$ of 0.93. This is very close to the commonly used FDOM pair (ex/em 370/460 nm), suggesting that use of in situ, single excitation-emission fluorometers may serve as a useful surrogate for DOC and DBP precursor concentrations. In addition to providing accurate information about DOC concentration and DBP precursor content, EEM's data provide useful information about DOM composition that helps elucidate changes in DOM source by site and date. Application of PARAFAC can be used to track specific components of the DOM pool. In this dataset, for example, the presence of C2 associated with terrestrial-derived humics was highly correlated to DBPFP.

Most utilities monitor raw and treated water TOC concentrations regularly and distribution system THMs and HAAs at least quarterly in compliance with USEPA regulations. However, these data are not always sufficient for detecting short-term or long-term changes in DOM amount or composition, which may impact drinking water quality. Furthermore, it is difficult to determine causes for unexpected increases in distribution system DBPs when information about source water quality is lacking. Use of optical measurements provides a way to monitor changes in both DOM amount and composition. These tools have the potential to be less expensive, faster, and more sensitive than laboratory chemical-based analyses (Henderson et al., 2009). Furthermore, the recent development of commercially available field instrumentation, which measures optical properties in situ, can provide real-time, continuous assessment of DOM (Downing et al., 2009, Saraceno et al., 2009). For example, using in situ optical sensors to measure water quality during a storm event (Saraceno et al. 2009) showed that peak DOC concentration lagged behind peak discharge by several hours. In cases where utilities have the ability to reduce intake water volumes for short periods of time, in situ optical sensors could be used to identify periods when such practices could be initiated.

This study highlights how measurement of optical properties has great potential to provide information about DOM dynamics in rivers. Understanding watershed sources of DOM and DBP precursors can help water utilities predict episodic and/or short-term events such as storm pulses and algal blooms, as well as seasonal patterns and long-term trends affecting drinking water quality. Such data will also help elucidate the effects of timber harvest, fire, development, and climate change on DOM export in forested watersheds. For drinking water utilities, understanding the location and timing of specific watershed sources of DBP precursors will help them optimize long-term source water protection programs. The ability to monitor the amount and composition of DOM entering treatment plants will facilitate successful and cost-effective treatment plant operations.

## Acknowledgments

This project was funded by the Eugene Water and Electric Board in collaboration with USGS. We thank the following people for their help with field work, laboratory analyses, and data processing—Steve Blair, Kurt Carpenter, Kathryn Crepeau, Jacob Fleck, Will Kerlin, John Franco Saraceno, and Travis von Dessonneck. The use of brand or firm names in this article is for identification purposes only and does not constitute endorsement by USGS.

## References

Aiken, G., and E. Cotsaris. 1995. Soil and hydrology: Their effect on NOM. J. Am. Water Resour. Assoc. 87:36–45.

Aiken, G., L.A. Kaplan, and J. Weishaar. 2002. Assessment of relative accuracy in the determination of organic matter concentrations in aquatic systems. J. Environ. Monit. 4:70–74.

Anderson, C. 2007. Influence of Cougar Reservoir drawdown on sediment and DDT transport and deposition in the McKenzie River basin, Oregon, water years 2002–04. USGS Scientific Investigations Report, 2007–5164. USGS, Reston, VA.

Anderson, C.A., and R. Bro. 2000. The N-way Toolbox for MATLAB. Chemom. Intell. Lab. Syst. 52:1–4.

Baker, A., R. Inverarity, M. Charlton, and S. Richmond. 2003. Detecting river pollution using fluorescence spectrophotometry: Case studies from the Ouseburn, NE England. Environ. Pollut. 124:57–70.

Belzile, C., C.S. Roesler, J.P. Christensen, N. Shakhova, and I. Semiletov. 2006. Fluorescence measured using the WETStar DOM fluorometer as a proxy for dissolved matter absorption. Estuarine Coastal Shelf Sci. 67:441–449.

Bergamaschi, B.A., E. Kalve, L. Guenther, G.O. Mendez, and K. Belitz. 2005. An assessment of optical properties of dissolved organic material as quantitative source indicators in the Santa Ana River Basin, Southern California. USGS Scientific Investigations Rep. 2005-5152. USGS, Reston, VA.

Boyer, E.W., G.M. Hornberger, K.E. Bencala, and D.M. McKnight. 1997. Response characteristics of DOC flushing in an alpine catchment. Hydrol. Processes 11:1635–1647.

Chow, A.T., S.-T. Lee, A.T. O'Geen, T. Orozco, D. Beaudette, P.-W. Wong, P.J. Hernes, K.W. Tate, and R.A. Dahlgren. 2009. Litter contributions to dissolved organic matter and disinfection byproduct precursors in California oak woodland watersheds. J. Environ. Qual. 38:2334–2343.

Coble, P.G. 2007. Marine optical biogeochemistry: The chemistry of ocean color. Chem. Rev. 107:402–418.

Cook, R.L., J.E. Birdwell, C. Lattao, and M. Lowry. 2009. A multi-method comparison of Atchafalaya Basin surface water organic matter samples. J. Environ. Qual. 38:702–711.

Cory, R.M., and D.M. McKnight. 2005. Fluorescence spectroscopy reveals ubiquitous presence of oxidized and reduced quinones in dissolved organic matter. Environ. Sci. Technol. 39:8142–8149.

Crepeau, K.L., M.S. Fram, and N. Bush. 2004. Method of analysis at the USGS California Sacramento Laboratory. Determination of trihalomethane formation potential, method validation, and quality control practices scientific investigations report 2004–5003. USGS, Reston, VA.

Croué, J.P., J.F. Debroux, G.L. Amy, G.R. Aiken, and J.A. Leenheer. 1999. Natural organic matter: Structural characteristics and reactive properties. p. 65–93. *In* P.C. Singer (ed.) Formation and control of disinfection by-products in drinking water. Am. Water Works Assoc., Denver, CO.

Croué, J.P., D. Violleau, and L. Lavouyrie. 2000. Disinfection by-product formation potentials of hydrophobic and hydrophilic natural organic matter fractions: A comparison between a low- and high-humic water. p. 139–153. *In* S.E. Barrett et al. (ed.) Natural Organic Matter and Disinfection By-Products: Characterization and Control in Drinking Water, Vol. ACS Symp. Series 761. Am. Chem. Soc., Washington, DC.

Dalzell, B.J., T.R. Filley, and J.M. Harbor. 2005. Flood pulse influences on terrestrial organic matter export from an agricultural watershed. J. Geophys. Res. 110:G02011, doi:10.1029/2005JG000043.

Downing, B.D., B.A. Bergamaschi, D.B. Evans, and E. Boss. 2008. Assessing contribution of DOC from sediments to a drinking-water reservoir using optical profiling. Lake Reservoir Manage. 24:381–391.

Downing, B.D., E. Boss, B.A. Bergamaschi, J.A. Fleck, M.A. Lionberger, N.K. Ganju, D.H. Schoellhamer, and R. Fujii. 2009. Quantifying fluxes and characterizing compositional changes of dissolved organic matter in aquatic systems in situ using combined acoustic and optical measurements. Limnol. Oceanogr. 7:119–131.

Edwards, T.K., and G.D. Glysson. 1999. Field methods for measurement of fluvial sediment: Techniques of water-resources investigations of the

USGS, Book 3, Chapter C2.

Edzwald, J.K., W.C. Becker, and K.L. Wattier. 1985. Surrogate parameters for monitoring organic matter and THM precursors. J. Am. Water Resour. Assoc. 77:122–132.

Engelage, S.K., and W.T. Stringfellow. 2009. Disinfection byproduct formation potentials of wetlands, agricultural drains, and rivers and the effect of biodegradation on trihalomethane precursors. J. Environ. Qual. 38:1901–1908.

HDR Engineering. 2007. Eugene Water and Electric Board lead and copper evaluation report. HDR Engineering, Bellevue, WA.

Helms, J.R., A. Stubbins, J.D. Ritchie, E.C. Minor, D.J. Kieber, and K. Mopper. 2008. Absorption spectral slopes and slope ratios as indicators of molecular weight, source, and photobleaching of chromophoric dissolved organic matter. Limnol. Oceanogr. 53:955–969.

Henderson, R.K., A. Baker, K.R. Murphy, A. Hambly, R.M. Stuetz, and S.J. Kahn. 2009. Fluorescence as a potential monitoring tool for recycled water systems: A review. Water Res. 43:863–881.

Hernes, P.J., R.G.M. Spencer, R.Y. Dyda, B.A. Pellerin, P.A.M. Bachand, and B.A. Bergamaschi. 2008. The role of hydrologic regimes on dissolved organic carbon composition in an agricultural watershed. Geochim. Cosmochim. Acta 72:5266–5277.

Hinton, M.J., S.L. Schiff, and M.C. English. 1997. The significance of storms for the concentration and export of dissolved organic carbon from two Precambrian Shield catchments. Biogeochemistry 36:67–88.

Hood, E., D.M. McKnight, and M.W. Williams. 2003. Sources and chemical character of dissolved organic carbon across an alpine/subalpine ecotone, Green Lakes Valley, Colorado Front Range, United States. Water Resour. Res. 39:1188, doi:10.1029/2002WR001738.

Hood, E., M.N. Gooseff, and S.L. Johnson. 2006. Changes in the character of stream water dissolved organic carbon during flushing in three small watershed, Oregon. J. Geophys. Res. 111:G01007, doi:10.1029/2005JG000082.

Hua, B., K. Veum, A. Kioirala, J. Jones, T. Clevenger, and B. Deng. 2007. Fluorescence fingerprints to monitor total trihalomethanes and N-nitrosodimethylamine formation potentials in water. Environ. Chem. Lett. 5:73–77.

Hua, G., and D.A. Reckhow. 2007. Characterization of disinfection byproduct precursors based on hydrophobicity and molecular size. Environ. Sci. Technol. 41:3309–3315.

Hudson, N., A. Baker, and D. Reynolds. 2007. Fluorescence analysis of dissolved organic matter in natural, waste and polluted waters: A review. River Res. Appl. 23:631–649.

Jaffe, R., D.M. McKnight, N. Maie, R. Cory, W.H. McDowell, and J.L. Campbell. 2008. Spatial and temporal variations in DOM composition in ecosystems: The importance of long-term monitoring of optical properties. J. Geophys. Res. 113:G04032, doi:10.1029/2008JG000683.

Jefferson, A. 2006. Hydrology and geomorphic evolution of basaltic landscapes, High Cascades, Oregon. Ph.D. diss., Oregon State Univ.

Krasner, S.W., H.S. Weinberg, S.D. Richardson, S.J. Pastor, R. Chinn, M.J. Sclimenti, G.D. Onstad, and A.D. Thurston. 2006. Occurrence of a new generation of disinfection byproducts. Environ. Sci. Technol. 40:7175–7185.

Kraus, T.E.C., B.A. Bergamaschi, P.J. Hernes, R.G.M. Spencer, R. Stepanauskas, C. Kendall, R.F. Losee, and R. Fujii. 2008. Assessing the contribution of wetlands and subsided islands to dissolved organic matter and disinfection byproduct precursors in the Sacramento-San Joaquin River Delta: A geochemical approach. Org. Geochem. 39:1302–1318.

Leenheer, J.A., and J.P. Croué. 2003. Characterizing dissolved aquatic organic matter. Environ. Sci. Technol. 37:18A–26A.

Liang, L., and P.C. Singer. 2003. Factors influencing the formation and relative distribution of haloacetic acids and trihalomethanes in drinking water. Environ. Sci. Technol. 37:2920–2982.

MacDonald, S.J.L., and H. Patterson. 1997. Improvement of inner filter effect correction based on determination of effective geometric parameters using a conventional fluorimeter. Anal. Chim. Acta 338:155–162.

McGlynn, B.L., and J.J. McDonnell. 2003. Role of discrete landscape units in controlling catchment dissolved organic carbon dynamics. Water Resour. Res. 39:1090, doi:10.1029/2002WR001525.

McKnight, D.M., E.W. Boyer, P.K. Westerhoff, P.T. Doran, T. Kulbe, and D.T. Andersen. 2001. Spectrofluorometric characterization of dissolved organic matter for indication of precursor organic material and aromaticity. Limnol. Oceanogr. 46:38–48.

Morgenstern, K., N. Toth, and D. Donahue. 2009. McKenzie River septic system assistance project final report. Eugene Water and Electric Board. Available at http://www.eweb.org/public/documents/water/septicFinalReport.pdf (verified 29 July 2010).

Nakajima, F., M. Hanabusa, and H. Furumai. 2002. Excitation-emission fluorescence spectra and trihalomethane formation potential in the Tama River, Japan. Water Sci. Technol. Water Supply 2:481–486.

Neff, J.C., J.C. Finlay, S.A. Zimov, S.P. Davydov, J.J. Carrasco, E.A.G. Schuur, and A.I. Davydova. 2006. Seasonal changes in the age and structure of dissolved organic carbon in Siberian rivers and streams. Geophys. Res. Lett. 33:L23401, doi:10.1029/2006GL028222.

Perry, S.A., and W.B. Perry. 1991. Organic carbon dynamics in two regulated rivers in northwestern Montana, USA. Hydrobiologia 218:193–203.

Reckhow D.A., Singer P.C., and R.L. Malcolm. 1990. Chlorination of humic materials: byproduct formation and chemical interpretations. Environ. Sci. Technol. 24:1655–1664.

Reckhow, D.A., P.L.S. Rees, and D. Bryan. 2004. Watershed sources of disinfection byproduct precursors. Water Sci. Technol. Water Supply 4:61–69.

Sanderman, J., K.A. Lohse, J.A. Baldock, and R. Amundson. 2009. Linking soils and streams: Sources and chemistry of dissolved organic matter in a small coastal watershed. Water Resour. Res. 45:W03418, doi:10.1029/2008WR006977.

Saraceno, J., B.A. Pellerin, B.D. Downing, E. Boss, P.A.M. Bachand, and B.A. Bergamaschi. 2009. High frequency in situ optical measurements during a storm event: Assessing relationships between dissolved organic matter, sediment concentrations and hydrologic processes. J. Geophys. Res. 114:G00F09, doi:10.1029/2009JG000989.

Schiff, S.L., R. Aravena, S.E. Trumbore, M.J. Hinton, R. Elgood, and P.J. Dillon. 1997. Export of DOC from forested catchments on the Precambrian Shield of Central Ontario: Clues from 13C and 14C. Biogeochemistry 6:43–65.

Sherrod, D.R., and J.G. Smith. 2000. Geologic map of Upper Eocene to Holocene volcanic and related rocks of the Cascade Range, Oregon. USGS, MAP I–2569

Singer, P.C. 1999. Humic substances as precursors for potentially harmful disinfection by-products. Water Sci. Technol. 40:25–30.

Spencer, R.G.M., A. Baker, J.M.E. Ahad, G.L. Cowie, R. Ganeshram, R.C. Upstill-Goddard, and G. Uher. 2007a. Discriminatory classification of natural and anthropogenic waters in two U.K. estuaries. Sci. Total Environ. 373:305–323.

Spencer, R.G.M., B.A. Pellerin, B.A. Bergamaschi, B.D. Downing, T.E.C. Kraus, D.E. Smart, R.D. Dahlgren, and P.J. Hernes. 2007b. Diurnal variability in riverine dissolved organic matter composition determined by in situ optical measurement in the San Joaquin River (California, USA). Hydrol. Processes 21:3181–3189.

Spencer, R.G.M., G. Aiken, K.P. Wickland, R.G. Striegl, and P.J. Hernes. 2008. Seasonal and spatial variability in dissolved organic matter quantity and composition from the Yukon River basin, Alaska. Global Biogeochem. Cycles 22:GB4002, doi:10.1029/2008GB003231.

Spencer, R.G.M., G. Aiken, K.D. Butler, M.M. Dornblaser, R.G. Striegl, and P.J. Hernes. 2009. Utilizing chromophoric dissolved organic matter measurements to derive export and reactivity of dissolved organic carbon exported to the Arctic Ocean: A case study of the Yukon River, Alaska. Geophys. Res. Lett. 36:L06401, doi:10.1029/2008GL036831.

SPSS Inc. 1998. SYSTAT for Windows, Version 8. SPSS, Evanston, IL.

Stedmon, C.A., S. Markager, and R. Bro. 2003. Tracing dissolved organic matter in aquatic environments using a new approach to fluorescence spectroscopy. Mar. Chem. 82:239–254.

Stedmon, C.A., and S. Markager. 2005. Tracing the production and degradation of autochthonous fractions of dissolved organic matter by fluorescence analysis. Limnol. Oceanogr. 50:1415–1426.

Stedmon, C.A., and R. Bro. 2008. Characterizing dissolved organic matter fluorescence with parallel factor analysis: A tutorial. Limnol. Oceanogr. 6:572–579.

Stepczuck, C., A.B. Martin, P. Longabucco, J.A. Bloomfield, and S.W. Effler. 1998. Allocthonous contributions of THM precursors to a eutrophic reservoir. Lake Reservoir Manage. 14:344–355.

Tague, C., and G.E. Grant. 2004. A geological framework for interpreting the low flow regimes of Cascade streams, Willamette River Basin, Oregon. Water Resour. Res. 40:W04303, doi:10.1029/2003WR002629.

Twardowski, M.S., E. Boss, J.M. Sullivanc, and P.L. Donaghay. 2004. Modeling the spectral shape of absorption by chromophoric dissolved organic matter. Mar. Chem. 89:69–88.

Unscrambler. 2005. The Unscrambler. Vers. 9.2. Camo Technologies, Oslo, Norway.

Vidon, P., L.E. Wagner, and E. Soyeux. 2008. Changes in the character of DOC in streams during storms in two Midwestern watersheds with contrasting land uses. Biogeochemistry 88:257–270.

Weishaar, J.L., G.R. Aiken, B.A. Bergamaschi, M.S. Fram, R. Fujii, and K. Mopper. 2003. Evaluation of specific ultraviolet absorbance as an indicator of the chemical composition and reactivity of dissolved organic carbon. Environ. Sci. Technol. 37:4702–4708.

Wu, W.W., P.A. Chadik, W.M. Davis, J.J. Delfino, and D.H. Powell. 2000. The effect of structural characteristics of humic substances on disinfection by-product formation in chlorination. p. 109–121. *In* S.E. Barrett et al. (ed.) Natural organic matter and disinfection by-products: Characterization and control in drinking water. ACS Symp. Series 761. Am. Chem. Soc., Washington, DC.